



‘Plug-and-Power’ Point-of-Care diagnostics: A novel approach for self-powered electronic reader-based portable analytical devices



Yaiza Montes-Cebrián^{a,*}, Lorena del Torno-de Román^b, Albert Álvarez-Carulla^a,
Jordi Colomer-Farrarons^a, Shelley D. Minter^c, Neus Sabaté^{b,d,e}, Pere Ll. Miribel-Català^a,
Juan Pablo Esquivel^b

^a Discrete-to-Integrated (D2In) Research Group, Department of Electronic and Biomedical Engineering, Faculty of Physics, University of Barcelona (UB), 1st Martí i Franquès St., 08028 Barcelona, Spain

^b Instituto de Microelectrónica de Barcelona IMB-CNM (CSIC), C/ del Tíllers, Campus Universitat Autònoma de Barcelona (UAB), 08193 Bellaterra, Barcelona, Spain

^c Department of Chemistry, University of Utah, 315 S 1400 E Room 2020, Salt Lake City, UT 84112, USA

^d Catalan Institution for Research and Advanced Studies (ICREA), Passeig Lluís Companys 23, 08010 Barcelona, Spain

^e Fuelium, Av. De Can Domenech – Edifici Eureka, Campus de la UAB, 08193 Bellaterra, Barcelona, Spain

ARTICLE INFO

Keywords:

Plug-and-Power
Self-powered
Paper-based
Glucometer
Low-power electronics

ABSTRACT

This paper presents an innovative approach in the portable Point-of-Care diagnostics field, the Plug-and-Power concept. In this new disposable sensor and plug-and-play reader paradigm, the energy required to perform a measurement is always available within the disposable test component. The reader unit contains all the required electronic modules to run the test, process data and display the result, but does not include any battery or power source. Instead, the disposable part acts as both the sensor and the power source. Additionally, this approach provides environmental benefits related to battery usage and disposal, as the paper-based power source has non-toxic redox chemistry that makes it eco-friendly and safe to follow the same waste stream as disposable test strips. The feasibility of this Plug-and-Power approach is demonstrated in this work with the development of a self-powered portable glucometer consisting of two parts: a test strip including a paper-based power source and a paper-based biofuel cell as a glucose sensor; and an application-specific battery-less electronic reader designed to extract the energy from the test strip, process the signal provided and show the glucose concentration on a display. The device was tested with human serum samples with glucose concentrations between 5 and 30 mM, providing quantitative results in good agreement with commercial measuring instruments. The advantages of the present approach can be extended to any kind of biosensors measuring different analytes and biological matrices, and in this way, strengthen the goals of Point-of-Care diagnostics towards laboratory decentralization, personalized medicine and improving patient compliance.

1. Introduction

Point of Care (POC) diagnostics have been proving their benefits in public global health over centralized laboratory diagnostics as they remove the constraints of requiring large healthcare infrastructures, complex medical equipment and well-trained technicians. POC devices allow monitoring of health conditions, reducing medical costs, as well as controlling infectious outbreaks, without the need of dedicated laboratory equipment. In addition, these devices offer the advantages of rapid results and patient proximity (Chan et al., 2017; Choi, 2016;

Drain et al., 2014; Wang et al., 2016a; Zarei, 2017; Yager et al., 2006). The development of portable POC diagnostics pursues the characteristics defined by the World Health Organization in the acronym ASSURED (affordable, sensitive, specific, user-friendly, rapid and robust, equipment free, and deliverable to users) to provide suitable solutions to even the lowest-resource global health settings (Fu et al., 2011). Despite the many advances in the field, equipment-free POC diagnostic devices still face important challenges related to reliability. The use of an electronic reader allows overcoming this aspect, as it provides an unambiguous qualitative/quantitative result of an assay and can

* Corresponding author.

E-mail addresses: ymontes@ub.edu (Y. Montes-Cebrián), lorena.deltorno@imb-cnm.csic.es (L. del Torno-de Román), albertalvarez@ub.edu (A. Álvarez-Carulla), jcolomerf@ub.edu (J. Colomer-Farrarons), minter@chem.utah.edu (S.D. Minter), nsabate@fuelium.tech (N. Sabaté), peremiribelcatala@ub.edu (P.L. Miribel-Català), juanpablo.esquivel@csic.es (J.P. Esquivel).

<https://doi.org/10.1016/j.bios.2018.07.034>

Received 3 May 2018; Received in revised form 13 July 2018; Accepted 16 July 2018

Available online 18 July 2018

0956-5663/ © 2018 Elsevier B.V. All rights reserved.

improve the sensitivity and the limit of detection.

The reader-disposable approach is predominantly used in the POC devices commercially available, and it is still the one mostly followed by initiatives undergoing research and development phases (Chin et al., 2012; Gervais et al., 2011; Zarei, 2017). These devices consist on a reusable electronic reader unit and a disposable part in the form of a strip, cartridge or card. The disposable test strip is used to collect the sample and transport it to the biosensor where the measurement is performed. After a single use, this strip is discarded avoiding cross-contamination. Depending on the detection principle and sample matrix to be detected, portable readers may also perform a variety of functions including for example sample pretreatment, hydraulic controls, heating, timing, light sources, photodetectors, electrochemical instrumentation, Radio frequency communications and, in most cases, displays as the interface between the device and the user to set up the test and show the result.

An example is the system presented by (Cruz et al., 2014). The authors present an approach capable of performing cyclic voltammetry for electrochemical immunosensing of cortisol. In contrast to the device presented here, the reported approach is not self-powered and, moreover, it does not have a custom-made design for the application since it uses a commercial miniaturized potentiostat on an evaluation board. However, the developed prototype is low-cost, portable and the analog front-end is based on a transimpedance amplifier (TIA).

To perform these functions, portable readers require a source of electrical power. This need has been fulfilled with either primary or secondary batteries. Regardless of their autonomy, batteries must be replaced or recharged periodically to maintain the device operation. This may seem a simple task in developed regions with reliable electric power grids and ubiquitous battery supplies. However, it can be quite challenging in low-resource settings, which is precisely where this kind of portable diagnostic devices are needed the most. Additionally, uncontrolled disposal of used batteries is becoming a severe problem in such regions of the world, as there is not only a lack of environmental regulations but also proper recycling facilities (Widmer et al., 2005; Larcher and Tarascon, 2015; Ongondo et al., 2011).

This paper presents a novel solution to the power requirements in the portable diagnostics field, the Plug-and-Power concept. We propose a plug-and-play reader-disposable device in which the energy required to perform a single test is always available within the disposable test component. In this case, the reader unit contains all the required electronic systems to run the test, including a display to visualize the result, but does not include any battery or power source. Instead, the disposable part acts as both the sensor and the power source. Additionally, this approach provides environmental benefits related to battery usage and disposal. The paper-based power source used for this approach has non-toxic redox chemistry that makes it eco-friendly and safe to follow the same waste stream as the disposable test strip or cartridge, including incineration, a typical outcome of those components that have been in contact with biological samples. The operation of this device, from the user perspective, is the same as for a conventional device, with the added advantage of not worrying about recharging it or where to recycle the used batteries. This approach strengthens the goals of Point-of-Care diagnostics towards laboratory decentralization, personalized medicine and improving patient compliance.

The applicability of this novel approach is demonstrated with the development of a self-powered portable blood glucometer, one of the Point-Of-Care applications that is already well-established in the market. Although many methods of glucose monitoring have been proposed (Fischer et al., 2016; Kulkarni and Slaughter, 2017; Lee et al., 2017; Narvaez Villarrubia et al., 2016; Slaughter and Kulkarni, 2016), the most widely used by both patients and healthcare professionals are the portable blood glucometers, as they are small, inexpensive, rapid and user-friendly (Wang et al., 2016a; Wang et al., 2016b; Zarei, 2017). These advantages are maintained in the presented Plug-and-Power

prototype, which consists of two parts: a test strip including a paper-based power source and a paper-based bio-fuel cell as the glucose sensor; and an application-specific battery-less electronic reader designed to extract the energy from the test strip, sample and process the signal provided by it and display the glucose concentration in the sample on a digital display.

2. Device concept and operation

The design and operation of the presented device resembles that of a typical commercial handheld glucometer, consisting of two parts: a disposable test strip and an electronic reader. However, this device introduces a new approach based on two main features: 1) the disposable test strip generates the electrical power used by the electronic reader to perform a measurement, and 2) the glucose concentration is measured by the reader from the output signal of a bio fuel cell, rather than using a classical solution based on a three-electrode configuration electrochemical cell.

The whole system is compact, lightweight and portable. The battery-less electronic reader has a size of $85.0 \times 42.0 \times 21.0$ mm, while the disposable test strip has a size of $20.0 \times 25.0 \times 1.8$ mm. From a user point of view, the device is easy to operate, as shown in Fig. 1. First, the strip is introduced in the reader. Then, the user adds the sample to the inlet of the test strip. Finally, the user can read the result of the test in the display of the smart electronic reader. After the measurement, the test strip can be safely discarded, while the electronic reader can be reused indefinitely for subsequent measurements.

The internal operation of the device can also be seen in Fig. 1. Once the liquid sample is added to the test strip, it flows by capillary action through a piece of paper. The sample diverges towards both ends of the paper, reaching on one side the power source, and on the other side, the sensor. The liquid activates the power source and the produced energy wakes up the electronic circuit in the reader. Then, the electronics regulate the power to a suitable working voltage of up to 3 V for the instrumentation. Afterwards, the circuit performs an amperometric glucose measurement using the sensor. The signal measured from the sensor is converted and processed to, finally, show on a display the quantitative result of glucose concentration contained in the sample.

2.1. Paper-based test strip

The disposable test strip is composed by two main components, a paper-based power source and a paper-based bio fuel cell acting as a glucose sensor. The components share a single paper strip of 5×20 mm that receives the sample in its middle zone and diverges it towards both ends. Fig. 2a shows a picture of the disposable test strip and Fig. 2b depicts an exploded view of its main components.

The paper-based power source has been customized by Fuelium Company for this application based on one of their batteries models LF55. This paper-based power source is composed of a paper membrane placed in contact with two electrodes. The proprietary electrode technology contains no heavy metals nor other toxic components, so it does not require special disposal considerations after its use. The batteries are only activated upon addition of an aqueous sample and provide a steady power output after being activated by either deionized water (D.I.) water or any physiological fluid such as plasma, serum, saliva, sweat or urine. Since these batteries only start their operation after activation with the liquid sample, they do not suffer from self-discharge during storage so their shelf life complies with the requirements of diagnostics test kits. For this application, the electrodes have been placed on top and bottom sides of a paper strip and the power source has been adjusted to provide an output voltage of 1.5 V and a minimum power of 10 mW for at least 20 min after being activated with a serum sample with a minimum volume of 12.5 μ L.

Instead of using a sensor based on a typical three-electrode configuration electrochemical cell, the glucose concentration is measured

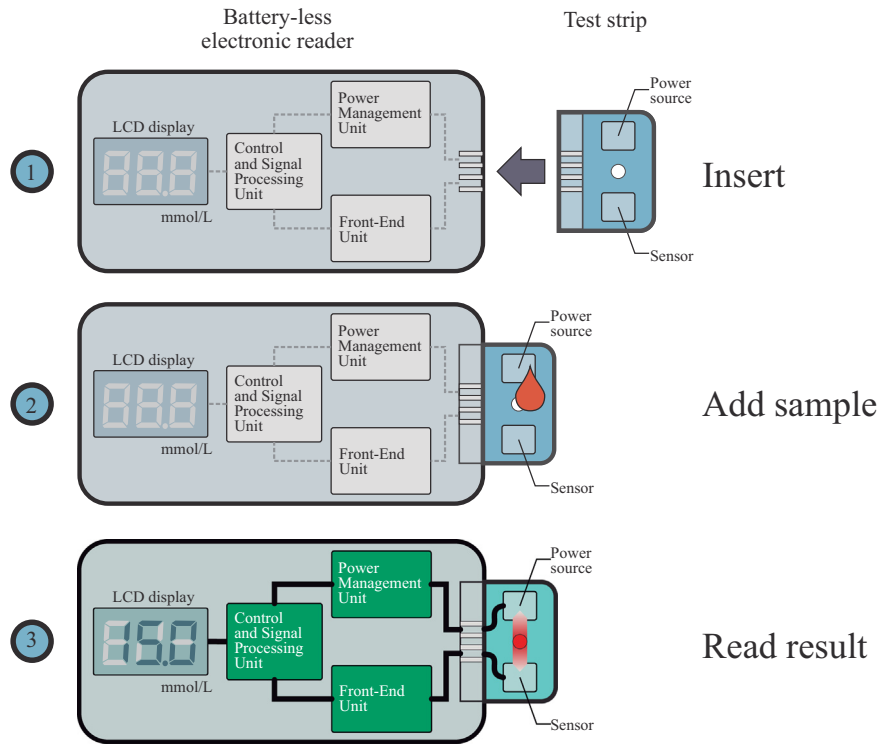


Fig. 1. Operation of Plug-and-Power Point-of-Care diagnostics device.

from the output signal of a paper-based enzymatic fuel cell. The device is composed of a glucose dehydrogenase (GDH) anode and a bilirubin oxidase (BOX) cathode placed on both sides of the paper strip. The fuel cell provides a response in power output that is proportional to the glucose concentration in the sample. This sensing method based in fuel cells response is used, for example, in many commercial breath alcoholmeters, known as breathalysers. It is a well-established and proven technique that is endorsed by industry and law-enforcement agencies worldwide (Leonard, 2012; Noordzij, 1975). In this case, the device performs a chronoamperometric measurement, subjecting the fuel cell to a fixed voltage while recording the produced current. All the electrodes are connected to silver tracks ink-jet printed on a plastic film.

The disposable strip components are assembled on top of an acrylic substrate to provide mechanical robustness.

2.2. Battery-less electronic reader

The electronic reader was conceived considering the particular features of this application. It was designed to operate with the voltage and power ranges provided by the paper-based power source and ensures robustness and portability. The block diagram of the electronic reader is depicted in Fig. 3. The disposable test strip provides the power that must be managed by the reader, and the signal to generate the glucose measurement.

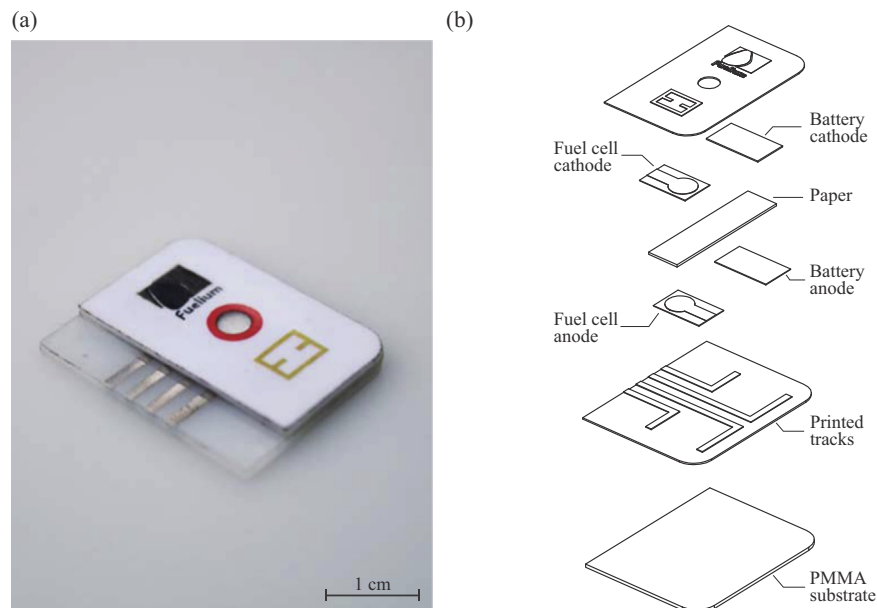


Fig. 2. a) Picture of paper-based test strip. b) Exploded view of its main components.

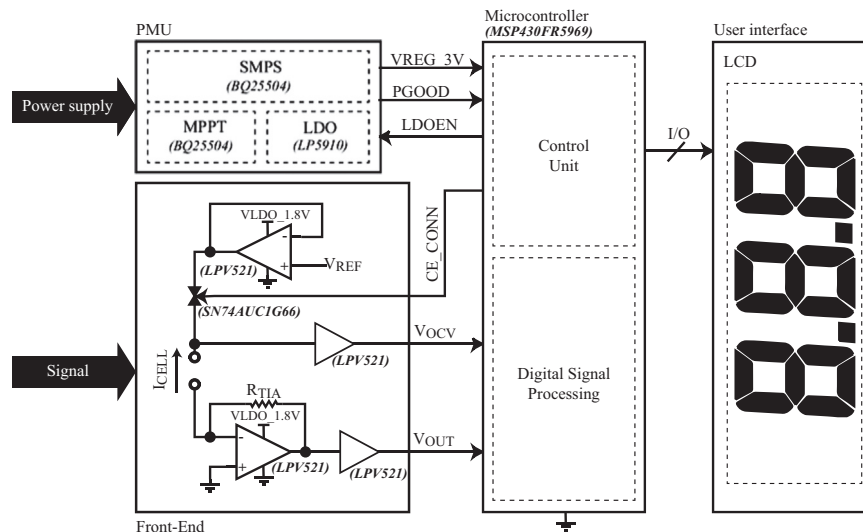


Fig. 3. Circuit of the battery-less electronic reader system.

The power supplied by the test strip goes to the Power Management Unit (PMU), where it is managed, and the control signals and voltage supplies of the system are generated. Meanwhile, the measurement signal, proportional to the concentration of glucose, is sent to the Front-End (FE) where the measurement is performed. Finally, the Control and Processing Unit (CPU), converts and processes the received information and sends it to a display, where the measurement result is shown.

2.2.1. Power management unit

The PMU is responsible for extracting and managing the available energy from the power source and offering a regulated output voltage in order to supply the different modules in the system. The PMU has been designed to work with the power provided by the disposable paper-based power source. In order to provide the necessary voltage to supply the components, a boost DC/DC converter in a cascade with a Low-Dropout (LDO) linear regulator are used. The first one boosts the voltage provided by the power source to 3.0 V (VREG_3V) to supply power to both the control and processing unit and the screen used to display the result. Meanwhile, the LDO provides a very stable 1.8 V (VLD0_1.8 V) regulated voltage with high noise rejection (Fig. 3). The 1.8 V is used to supply the analog block composed by the front-end module, which needs a very stable and well-regulated voltage supply with high noise rejection to avoid the effect of the inherent switching noise at the output of the boost converter and the effect of transient voltage variations at the power supply. The regulated voltage levels were selected in order to be able to supply common Components off-the-shelf (COTS) parts, where 3.0 V is a typical voltage supply for digital parts (as microcontrollers or Analog-to-Digital Converters (ADC)) and 1.8 V, for low-voltage analog COTS parts (as Operational Amplifiers (OpAmp) or bandgap references).

Furthermore, the PMU has a Maximum Power Point Tracking (MPPT) module, which ensures that the energy is extracted efficiently from the power source, i.e. when the system demands energy from the power source, it extracts the maximum power that the power source is able to deliver at that moment. Thus, the solution can attend punctual high-power requirements coming from the different modules and shorten the required start-up time. To achieve that, the MPPT modulates the input impedance of the boost converter and sets the power source operating point to that with output voltage of 0.7 V, where the power source is able to provide the maximum power.

This module also provides some additional features that enable the system to perform a smart power management carried out by the microcontroller. The boost converter outputs a signal called *PGOOD*. This is a low-level signal by default that changes to a high voltage level, as a

flag, when the voltage outputted by the boost converter reaches a voltage of 2.9 V. When regulated voltage drops under 2.4 V, the signal goes to low voltage level. This way, the microcontroller, able to operate with a minimum voltage supply of 1.8 V, can (dis)enable the LDO through a *LDOEN* signal or manage its different Ultra-Low-Power Modes (LPMs) to adapt the system operation to the available energy.

2.2.2. Front-end

In order to measure the current provided by the sensor, which is proportional to the glucose concentration, a potentiostat amplifier has been implemented. The potentiostat circuit can be divided into two stages. The first stage is responsible for setting the working voltage of the sensor. Based on the fuel cell characterization, it was obtained the working voltage where the sensor has the highest sensitivity to discriminate between glucose concentrations. During operation, this working voltage is generated using a voltage divider and a buffer amplifier. The second stage performs the current readout and translates this current into voltage using a transimpedance amplifier (TIA) stage. The TIA translates the current signal provided by the sensor (I_{CELL}) into a voltage signal by means of a resistor (R_{TIA}). The output signal (V_{OUT}) obtained at the output of the amplifier is proportional to the current provided by the strip. The equation that relates the output voltage and the current proportional to the glucose concentration is shown in the following equation:

$$V_{OUT} = R_{TIA} \cdot I_{CELL} \quad (1)$$

2.2.3. Control and Processing Unit

The system is managed through the CPU. It has been chosen an ultra-low-power microcontroller that needs only 1.8 V as minimum voltage to operate. This device has different operating modes: one active mode and seven software-selectable low-power modes. An interruption event wakes up the microcontroller from low-power mode. Then, the relevant tasks or operations are performed, and finally the microcontroller restores back to the low-power mode on return from the interrupt program. The microcontroller has been selected, because it presents an ultra-low-power system architecture that increases performance at lowered energy budgets, and an ultra-low-power 16-bit control processing unit and intelligent peripherals to extend the autonomy of the system.

For this application two ADC have been used to capture two analog signals. One is the open-circuit voltage of the fuel cell (OCV), which allows to know if the sensor is ready to perform the measurement. The other one is the measurement signal (V_{OUT}) related to the current across

the fuel cell (I_{CELL}), which is proportional to the glucose concentration. Some General Purpose Input/Output (GPIO) pins have been used in order to manage and control the PMU module and the display interface.

The conversion of the measured current to a glucose concentration has been carried out by means of a Lookup Table (LUT) (Bengtsson, 2012).

To manage the system, the microcontroller has been programmed to perform the next tasks. Initially, when the voltage supply provided by the boost converter reaches the 1.8 V needed to start its operation, it configures a GPIO pin connected to *PGOOD*. This pin will monitor the state of the regulated voltage supply. Meanwhile, the LDO is disabled using the *LDOEN* signal and the microcontroller goes to LPM to minimize power consumption. When *PGOOD* goes high, meaning that the regulated voltage supply has reached the 2.9 V, and enough energy is harvested to start the application operation, the microcontroller exits the Low-Power Mode (LPM) and starts to configure the different peripherals that are used.

Once the system is initialized, the microcontroller monitors the OCV of the fuel cell to check if the sample is available and start the measurement. If that is the case, it enables the LDO and starts the chronoamperometry, connecting the counter electrode through the *CE_CONN* signal. During this time, the microcontroller remains in LPM. After the selected time, the microcontroller exits the LPM, outputs the concentration measurement to the display and returns to LPM.

2.2.4. Display output

A commercial 7-Segments Liquid Crystal Display (LCD) has been used to show glucose concentration result due to its low power consumption. The numeric LCD used can display up to 3 digits. In order to facilitate connection and control of the LCD, an integrated circuit has been used, which reduces the number of control signals needed to control the display. The total consumption of this module is 0.33 μA at 3 V.

2.3. System integration and assembly

A scheme and picture of the whole system are shown in Fig. 4. The exploded view shows the placement of the different electronic blocks comprising the system, the connector for the disposable test strip, and the 3D printed casing. A Printed Circuit Board (PCB) with dimensions of 77 mm \times 32 mm was designed and implemented.

3. Material and methods

3.1. Chemicals and materials

All chemicals and biochemicals were, unless otherwise stated, purchased from Sigma-Aldrich. Human serum (H4522, Lot # SLBQ9160V) from human male AB plasma, USA origin, sterile-filtered, was used to validate the operation of the device. Phosphate buffer at pH 7.4 was utilized in preliminary validation studies. It was prepared by the combination of sodium phosphate monobasic dihydrate ($\text{NaH}_2\text{PO}_4 \cdot 2\text{H}_2\text{O}$), sodium phosphate dibasic dihydrate ($\text{Na}_2\text{HPO}_4 \cdot 2\text{H}_2\text{O}$) and potassium chloride (KCl) for a final 100 mM concentration. Glucose solutions were allowed to mutarotate for 24 h and were kept refrigerated at 4 °C until use. Tetrabutylammonium bromide (TBAB)-modified Nafion was prepared as previously reported. (Klotzbach et al., 2006) Flavin adenine dinucleotide-dependent glucose dehydrogenase (FAD-GDH, E.C. 1.1.99.10, GLDE-70-1192, *Aspergillus* sp.) was purchased from Sekisui Diagnostics (Lexington, MA, USA) and used as received. Bilirubin oxidase (BOx, E.C. 1.3.3.5, *Myrothecium* sp., BO-3) was obtained from Amano Enzyme Inc. (Japan) and used as received. Glucose oxidase from *Aspergillus niger* (EC 1.1.3.4, Type X-S, 175 units/mg of solid, 75% protein) and 5% by wt. Nafion EW1100 suspension were purchased from Sigma-Aldrich and used as received. Carboxylated MWCNT and hydroxylated MWCNTs were purchased

from cheaptubes.com.

Standard 14 papers were purchased from GE Healthcare, Pittsburgh, PA, USA. The main structure of the test strip was constructed from pressure sensitive adhesives (PSA) (Adhesives Research) and poly(methylmethacrylate) (PMMA) (Plexiglas, Evonik Performance Materials GmbH, Harmstadt, Germany).

Silver ink (LOCTITE ECI 1011, Henkel, Dusseldorf, Germany) and carbon ink (C2030519P4, Gwent Electronic Materials Ltd., Pontypool, Wales) were used to print the base electrodes for the fuel cell onto a polyethylene terephthalate (PET) substrate. The test strip conducting tracks were ink-jet printed using silver ink (PE410, DuPont, Bristol, UK) on a 125 μm polyethylene naphthalate (PEN) sheet (Teonex, DuPont, Chester, VA, USA). Paper-based power source electrodes were provided by Fuelium (Barcelona, Spain). All electronics components used for the electronic reader were purchased from Farnell (Madrid, Spain).

3.2. Device fabrication

The test strip structural components were designed with CorelDraw software (Corel, Ottawa, ON, Canada). Paper, PSA sheets and PMMA were cut with a CO₂ laser cutter (Mini 24, Epilog Laser, Golden, CO, USA).

The fuel cell configuration was adapted from the one reported in (del Torno-de Román et al., 2018). The fuel cell base electrodes were prepared by screen-printing onto a PET substrate. Initially, a track of silver ink was printed to improve conductivity. Following this, a carbon ink was screen printed on top of the silver layer in order to produce a rounded working electrode surface of 4-mm diameter. The screen-printed substrate was cut in segments of 5 mm \times 9 mm, each containing a single electrode. The active area of the screen-printed electrodes was then functionalized with the corresponding enzymatic ink for anode and cathode. The fuel cell anodes were prepared by adding 1.5 mg of FAD-GDH (30 mg mL⁻¹) enzyme to 75 μL of a 0.2 M citrate/phosphate buffer in ultrapure water. The crosslinker ethylene glycol diglycidyl ether (EGDGE) is diluted in ultrapure water to a concentration of 10% v/v. COOH-MWCNTs are added to isopropanol at a concentration of 5 mg mL⁻¹ and sonicated for 1 h. Naphthoquinone-Linear poly(ethyleneimine) (NQ-LPEI) was prepared as described in (Milton, 2017) and diluted at a concentration of 10 mg mL⁻¹ in ultrapure water. In an Eppendorf tube, 67% v/v of the NQ-LPEI solution, 30% v/v of the enzyme and 3% v/v of the cross-linker solution (EGDGE) are combined. 8.5 μL of the combined mixture is deposited on the surface of the electrode and left to dry overnight at room temperature. The fuel cell cathodes were modified by suspending 1.5 mg of BOX in 75 μL of 0.2 M citrate/phosphate buffer. 75 μL of the solution is added to 7.5 mg of Ac-MWCNTs as described in (Meredith et al., 2011; Milton et al., 2015). The solution is vortex mixed for 1 min, followed by 15 s of sonication: this procedure is repeated a total of 4 times. To this mixture, 25 μL of TBAB-Nafion suspension is added, followed by another vortex/sonication step. 33 μL of the mixture is then drop coated onto the surface of the screen-printed electrode and left to dry under a fan for 1.5–2 h. Both anodes and cathodes are stored at 4 °C when not in use.

A modified version of LF55 paper-based power source from Fuelium was adapted to the test strip. The anode and cathode power source electrodes were customized for this application considering the sample type, volume and power requirements. Each electrode had dimensions of 5 mm \times 9 mm, with a projected electroactive surface of 5 mm \times 5 mm. The conducting tracks of the test strip were ink-jet printed using Ag ink on a PEN sheet with a Cera Printer X-serie (Ceradrop, Limoges, France). Silver conducting paste was used for interconnection of fuel cell and power source electrodes to the conducting tracks. All the test strip components were manually assembled layer by layer using an acrylic alignment holder.

The electronic circuit of the battery-less reader was first simulated using Multisim software (National Instruments, Austin, Texas, United States). Ultiboard program (National Instruments, Austin, Texas, United

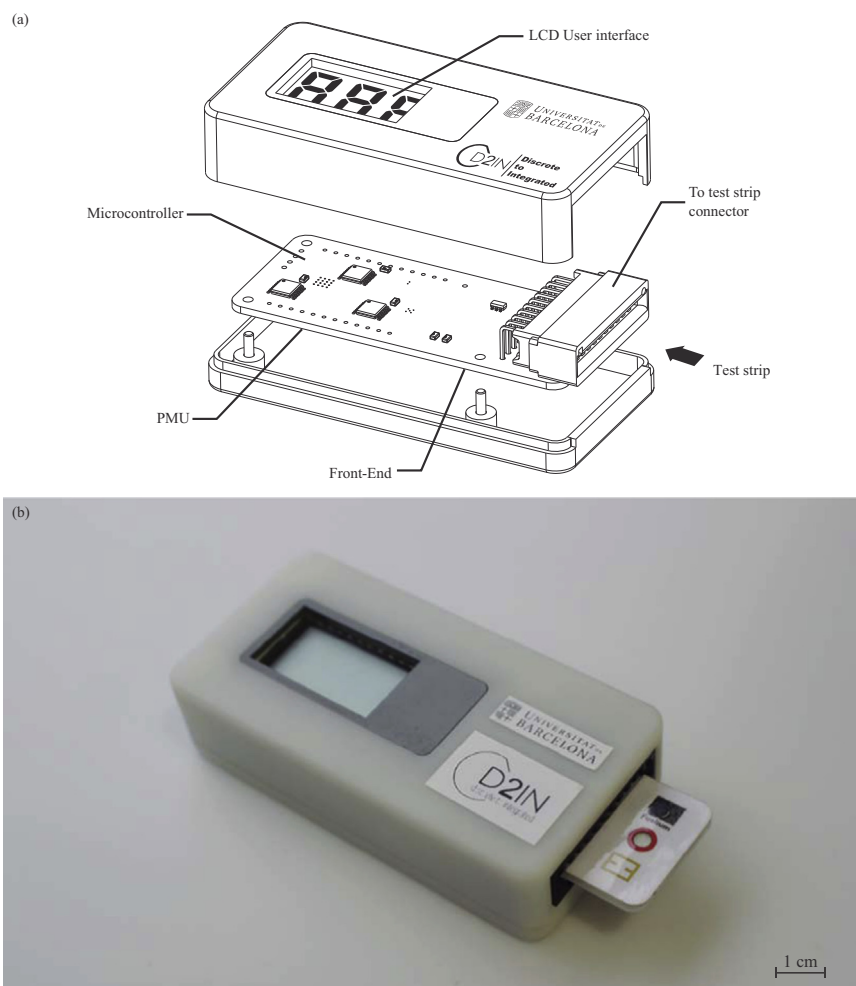


Fig. 4. a) Schematic of the system assembly. b) Photograph of the system.

States) was used to design the printed circuit board. The reader casing was designed using DesignSpark Mechanical.

3.3. Electronic and electrochemical characterization and validation

All electrochemical experiments were carried out with an Autolab PGSTAT204 (Metrohm, NL). For fuel cell and power source characterization, the open-circuit voltage of the fuel cell (OCV) of each cell was measured before polarization. Polarization curves were performed in potentiodynamic mode at a scan rate of 5 mV s^{-1} . Chronoamperometric curves of fuel cells were measured at 0.45 V for each glucose concentration.

The electronic validation and characterization were performed with a Source Measurement Unit (SMU) B2962A by Keysight Technology (USA) and an Agilent Technologies oscilloscope MSO-X 3034A (USA). Initial electronic characterization was carried out simulating the electrical behavior of the test strip via the SMU. The output voltage of the potentiostat was captured for different current curves corresponding to different glucose concentrations.

4. Results and discussion

4.1. Test strip characterization

The power source polarization curve was obtained after depositing $50 \mu\text{L}$ of serum at the inlet pad of the consumable test strip. In order to see its performance in time, discharge curves at 1 and 10 mA were also recorded. Fig. 5a and b show the obtained results. The power source

shows its capability of delivering 1 mA for at least 40 min (far beyond the typical operating time of point-of-care devices) whereas at 10 mA it sustained a voltage above 1.25 V for at least 5 min .

Bioelectrocatalysis of fuel cell electrodes was validated with half-cell voltammetric characterization. Figs. S1, S2 show representative voltammograms of bioanode and biocathode, respectively. Next, the glucose fuel cell of the test strip was characterized with human serum at different glucose concentrations. Serum as-purchased had a glucose concentration of 4.8 mM . A solution of 1 M glucose in 100 mM PBS buffer was prepared and spiked into the serum sample in order to increase glucose concentration while minimizing dilution of the original biological sample. Fig. 5c shows the polarization curves obtained at different glucose concentrations. From these I-V curves, it could be seen that the highest sensitivity is obtained between 0.35 and 0.50 V . Therefore, it was decided to polarize the fuel cell at 0.45 V to obtain the chronoamperometry curves of the fuel cell and sense glucose concentration. The currents generated by the fuel cell biased at 0.45 V were measured for 80 s , recording a variability below 15% for each of the glucose concentrations in serum. Mean chronoamperometric curves are depicted in Fig. 5d.

4.2. Battery-less electronic reader validation and characterization

All electronic modules introduced in Section 2.2 were fully characterized and validated individually as a prior step to the total integration of the system shown in Fig. 4. This individual characterization of the full-custom electronics was carried out following a two-phase testing procedure: Phase 1) an initial step using a SMU (section 3.3) to

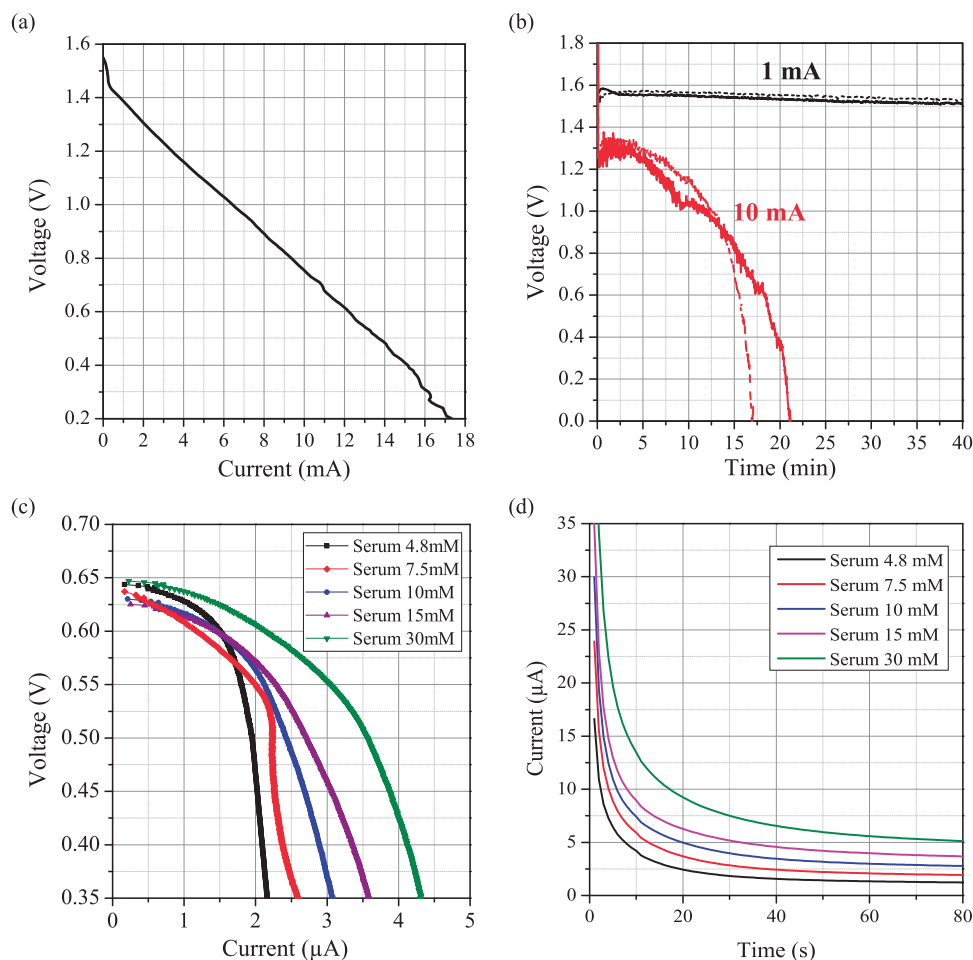


Fig. 5. Characterization of the Fuelium LF55 paper-based power source activated with serum samples. a) I-V paper-based power source characteristic. b) Paper-based power source discharge curves at 1 and 10 mA. Characterization of glucose fuel cell integrated in the test strip with different glucose concentrations in serum. c) Fuel cell polarization curves. d) Fuel cell chronoamperometry curves at 0.45 V.

simulate the electrical response/behavior of the test strip; and Phase 2) a second phase using real test strips. Upon successful completion of these two phases, the implementation, integration and validation of the full system (Fig. 4) was done. In such a way, the final assembly was programmed, calibrated to work with the given sensor and validated with real test strips in the final test procedure (Phase 3).

It is important to underline the accurate design of the front-end module to reduce the deviation error of the measurement through it. This error was derived as the difference between the injected current and the current measured through the full-custom electronic module. The electronic system was validated and a final error lower than 1% was verified in test phase 1 with a test strip simulated current produced by the SMU unit and in phase 2 using test strips.

From calibration phase (Phase 3), it was obtained that the electronic reader is able to measure currents up to 30 μA with a resolution of 13 nA. Fig. 6a shows the accuracy of the electronic reader. The electronic reader error is lower than 1.8%. This error depends on the ADC quantification error and the passive component tolerances.

The main effort was to settle the appropriate time to extract the measurement. This point was defined in terms of device resolution and the uncertainty related to the electronics. In this sense, the reader was programmed to measure the current corresponding to a given glucose concentration. In order to characterize the whole system and determine the precise time to extract the measurement, the consumable test strip was connected to the reader and fed with 50 μL of serum at different glucose concentrations between 5 and 30 mmol/L (same considerations as section 4.1).

The currents generated by the glucose fuel cell biased at 0.45 V were measured and recorded by the reader for 80 s. As seen in Fig. 6b, the current measured by the reader (I_{CELL}) virtually match with the chronoamperometry curves presented in Fig. 5d obtained with a commercial potentiostat (Autolab PGSTAT2014). These results allow to validate the operation of the reader and disposable strip system. As expected, the main difference between the curves measured by both instruments was identified for currents larger than 30 μA where the full-custom reader presents a maximum current detection limit, saturating for any higher value.

The chronoamperometric curves shown in Fig. 6b were used to define three operation regions (A, B and C) based on two criteria: the device resolution and the uncertainty in the time of measurement. These regions were used to determine the time to perform the measurement of current after submitting the fuel cell to the bias voltage.

The first criterion, device resolution, depends mainly on the sensor sensitivity and the electronic reader resolution. Based on the data from Fig. 6b, the sensor presents a higher sensitivity in region A whereas the lowest sensitivity is obtained in region C due to its decrease rate over time. On the other side, the electronic reader resolution is defined by the ADC resolution with a time-invariant value of 13 nA, negligible compared to the sensor sensitivity. According to this analysis, region C was ruled out to settle the time to extract the measurement.

The next step was the study of the measurement uncertainty to accurately define the time of the measurement. As it is shown in Fig. 6b, the chronoamperometry has a decreasing exponential response. This response excludes region A to carry out the measurement. In this

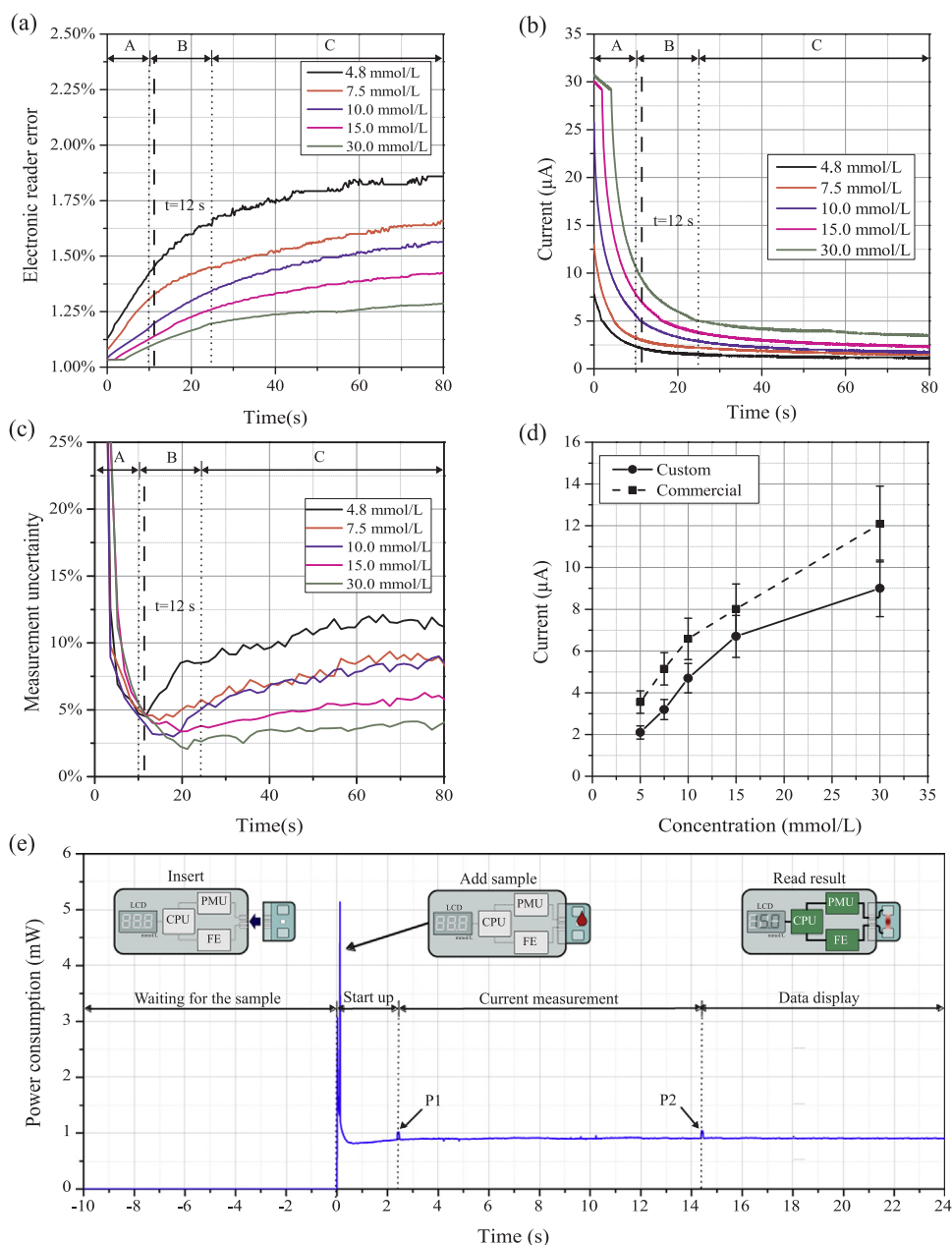


Fig. 6. a) Electronic reader current error. b) Chronoamperometry curves done with the battery-less electronic reader. c) Uncertainty in current measurement produced by the electronic reader. d) Transfer function that relates the current captured by the electronic reader with the glucose concentration and comparison against a commercial potentiostat (Autolab PGSTAT204). f) Temporal evolution of the electronic reader power consumption.

region, a small instability in the measurement time instant causes an important uncertainty in current measurement. Therefore, region B is the best region to perform the measurement. At this point, the current uncertainty in time was calculated (Fig. 6c) to establish the best time to extract the measurement within region B. The uncertainty is based on a 0.5 s range defined by the measurement sampling period of the processing unit. It was obtained that the best time to carry out the measurement is at 12 s, because it presents an electronics' uncertainty lower than 5% for the lowest glucose concentration.

A Lookup Table (LUT) (Bengtsson, 2012) based technique was used to translate the current value into the glucose concentration. Fig. 6d shows the transfer function that relates the current captured by the electronic reader with the glucose concentration and compares it against the one measured with the commercial potentiostat (Autolab PGSTAT204). Error bars in both curves account for the variability of the glucose sensor. As it can be seen, the data are proportional and only a

slight shift between the curves is presented. This is caused by the initial current saturation peak but, due to its systematic behavior, it is adjusted by a LUT in the postprocessing at the control unit.

Finally, Fig. 6e shows the operation phases of the system and the temporal evolution of the power consumption. The electronic reader is switched on when the serum sample is introduced into the disposable test strip, defining the start-up of the system. At this moment ($t = 0$ s), the typical inrush current peak takes place, reaching a value of up to 5 mW. Then, the reader enters into a low power mode, consuming just 900 μ W. It should be noted that the total electronics power consumption is much lower than the maximum power that the paper-based power source is able to supply, above the 10 mW. During this phase, the system waits in the low power mode of operation until the voltage provided by the disposable is stable. Then, the front-end module is switched on, the measurement is started and maintained during 12 s, which is labeled as the Current measurement phase. Finally, in the Data

display phase, the reader returns to the low power mode and the numerical result is displayed. Two small current peaks take place during the device operation. The first peak (P1) occurs when the front-end module is activated and the second (P2) when the measurement data is acquired and displayed. The result of the glucose concentration measurement is displayed on the screen until the disposable component is removed or it runs out of power after a few hours.

Significant research efforts have been made to develop systems which generate energy while monitor the glucose of a sample (Lee et al., 2017; Slaughter and Kulkarni, 2017). Nevertheless, the proposed systems do not have any electronics module to display the result, and it is necessary an external system to show it. Furthermore, accurate commercial glucometers are available, which just need a small sample volume to perform the measurement (Rajendran and Rayman, 2014). However, they require batteries which become hazardous waste and pose threats to health and the environment if improperly disposed. The novel battery-less system presented in this paper provides quantitative data, besides having a reusable reader and a disposable test-strip, acting as sensor and a power source, which does not contain any toxic material, so it can be safely disposed of after its use without the need of recycling.

5. Conclusions

This work presents the Plug-and-Power concept, a novel approach of powering portable Point-Of-Care devices that offers several advantages. In this case, the disposable test strip provides the energy needed to run an electronic reader and perform the test, defining a self-powered plug-and-play POC.

In this case, the developed system is able to monitor glucose and process and display the data without the need to either recharge or replace the batteries, as the energy to run a measurement is always available within the test strip. Additionally, this approach provides environmental benefits related to battery usage and disposal, as uncontrolled battery disposal leads to severe environmental pollution. The paper-based power source used for the present approach does not contain any toxic material, so it can be safely disposed of after its use without the need of recycling. Therefore, this eco-friendly power source can follow the same waste stream as a test strip that has been in contact with biological samples.

The results show that the battery-less reader is able to operate and manage the power provided by the paper-based power source integrated in the consumable test strip. In addition, the electronic reader performs an electrochemical detection, process the output signal of the sensor and express the result on a display. The electronic reader designed is able to measure currents up to 30 μ A with a resolution of 13 nA and an error below 1.8%. Due to the low power design of the reader that consumes only 900 μ W in low power mode, it is possible to perform the measurement with the power provided by the test strip, which is above the 10 mW. This shows that the self-powered device could be further improved to include additional functionalities for sample preparation or a wireless communications module to visualize the results on a laptop or even on a smartphone. A big challenge would be to integrate the electronic system into a single chip, making possible develop a flexible and totally disposable system.

The advantages of this approach were here demonstrated with the development of a portable glucometer, but this concept can be extended to other kinds of electrochemical sensors measuring other analytes and/or other biological matrices (Chin et al., 2012; da Silva et al., 2017; Kaushik et al., 2018; Wan et al., 2013). Moreover, this can also benefit

portable electronic analytical devices beyond clinical diagnostics, as for example the veterinary or environmental fields.

Acknowledgements

We would like to acknowledge I. González-Valls from Fuelium, S.L. for guidance in paper-battery handling and operation. Also, the authors would like to thank the support of the MINAUTO Project (TEC2016-78284-C3-3-R and TEC2016-78284-C3-1-R), Ministerio de Economía, Industria y Competitividad – Agencia Estatal de Investigación, and Fondo Europeo de Desarrollo Regional (AEI/FEDER, UE). N. Sabaté would like to thank the financial support received from ERC Consolidator Grant (SUPERCCELL - GA.648518). S.D. Minter would like to thank the financial support of the United States Department of Agriculture NIFA program (11322204).

Appendix A. Supporting information

Supplementary data associated with this article can be found in the online version at doi:10.1016/j.bios.2018.07.034.

References

- Bengtsson, L.E., 2012. *J. Sens. Technol.* 02, 177–184.
- Chan, H.N., Tan, M.J.A., Wu, H., 2017. *Lab Chip* 17, 2713–2739.
- Chin, C.D., Linder, V., Sia, S.K., 2012. *Lab Chip* 12, 2118.
- Choi, S., 2016. *Biotechnol. Adv.* 34, 321–330.
- Cruz, A.F.D., Noreña, N., Kaushik, A., Bhansali, S., 2014. *Biosens. Bioelectron.* 62, 249–254.
- Drain, P.K., Hyle, E.P., Noubary, F., Freedberg, K.A., Wilson, D., Bishai, W.R., Rodriguez, W., Bassett, I.V., 2014. *Lancet Infect. Dis.* 14, 239–249.
- Fischer, C., Fraiwan, A., Choi, S., 2016. *Biosens. Bioelectron.* 79, 193–197.
- Fu, E., Yager, P., Floriano, P.N., Christodoulides, N., McDevitt, J.T., 2011. *IEEE Pulse* 2, 40–50.
- Gervais, L., de Rooij, N., Delamarche, E., 2011. *Adv. Mater.* 23, H151–H176.
- Kaushik, A., Yndart, A., Kumar, S., Jayant, R.D., Vashist, A., Brown, A.N., Li, C.-Z., Nair, M., 2018. *Sci. Rep.* 8, 9700.
- Klotzbach, T., Watt, M., Ansari, Y., Minter, S.D., 2006. *J. Membr. Sci.* 282, 276–283.
- Kulkarni, T., Slaughter, G., 2017. *Proc. IEEE Sens.*
- Larcher, D., Tarascon, J.-M., 2015. *Nat. Chem.* 7, 19–29.
- Lee, I., Sode, T., Loew, N., Tsugawa, W., Lowe, C.R., Sode, K., 2017. *Biosens. Bioelectron.* 93, 335–339.
- Leonard, R.J., 2012. *J. Forensic Sci.* 57, 1614–1620.
- Meredith, M.T., Minson, M., Hickey, D., Artyushkova, K., Glatzhofer, D.T., Minter, S.D., 2011. *ACS Catal.* 1, 1683–1690.
- Milton, R.D., Lim, K., Hickey, D.P., Minter, S.D., 2015. *Bioelectrochemistry* 106, 56–63.
- Milton, R.D., 2015. FAD-Dependent glucose dehydrogenase immobilization and mediation within a naphthoquinone redox polymer. In: In: Minter, S. (Ed.), *Enzyme stabilization and immobilization. Methods in molecular biology* 1504 Humana Press, New York, NY. https://doi.org/10.1007/978-1-4939-6499-4_15.
- Narvaez Villarrubia, C.W., Soavi, F., Santoro, C., Arbizzani, C., Serov, A., Rojas-Carbonell, S., Gupta, G., Atanassov, P., 2016. *Biosens. Bioelectron.* 86, 459–465.
- Noordzij, P.C., 1975. *Alcohol Drugs Traffic Saf.* 553–560.
- Ongondo, F.O., Williams, I.D., Cherrett, T.J., 2011. *Waste Manag.* 31, 714–730.
- Rajendran, R., Rayman, G., 2014. *J. Diabetes Sci. Technol.* 8, 1081–1090.
- da Silva, E.T.S.G., Souto, D.E.P., Barragan, J.T.C., de F. Giarola, J., de Moraes, A.C.M., Kubota, L.T., 2017. *ChemElectroChem* 4, 778–794.
- Slaughter, G., Kulkarni, T., 2016. *Biosens. Bioelectron.* 78, 45–50.
- Slaughter, G., Kulkarni, T., 2017. *Sci. Rep.* 7, 1471.
- del Torno-de Román, L., Navarro, M., Hughes, G., Esquivel, J.P., Milton, R.D., Minter, S.D., Sabaté, N., 2018. *Electrochim. Acta* 282, 336–342.
- Wan, Y., Su, Y., Zhu, X., Liu, G., Fan, C., 2013. *Biosens. Bioelectron.* 47, 1–11.
- Wang, S., Lifson, M.A., Inci, F., Liang, L.-G., Sheng, Y.-F., Demirci, U., 2016a. *Expert Rev. Mol. Diagn.* 16, 449–459.
- Wang, S.Q., Chinnasamy, T., Lifson, M.A., Inci, F., Demirci, U., 2016b. *Trends Biotechnol.*
- Widmer, R., Oswald-Krapf, H., Sinha-Khetriwal, D., Schnellmann, M., Böni, H., 2005. *Environ. Impact Assess. Rev.* 25, 436–458.
- Yager, P., Edwards, T., Fu, E., Helton, K., Nelson, K., Tam, M.R., Weigl, B.H., 2006. *Nature-Lond.* 442, 412.
- Zarei, M., 2017. *TrAC - Trends Anal. Chem.*